Proceedings of 2004 IEEE/RSJ International Conference on
Intelligent Robots and Systems
September 28 - October 2, 2004, Sendai, Japan

Quantitative Comparison of Bilateral Teleoperation Systems Using $\mathcal{H}_\infty$ Framework

Keehoon Kim† M. Cenk Cavusoglu‡ Wan Kyun Chung†

† Robotics & Bio-Mechatronics Lab., Pohang Univ. of Science and Technology(POSTECH) , Pohang, Korea
E-mail : {khk,wkchung}@postech.ac.kr

‡ Dept. of Electrical Engineering and Computer Science, Case Western Reserve Univ., Cleveland, OH, USA
Email : cavusoglu@cwru.edu

***Abstract*— Since teleoperation systems are mostly executed in the extreme environment, there are constraints in designing the mechanism and choosing sensors. This paper presents a novel *quantitative* comparison method of teleoperators based on $\mathcal{H}_\infty$ framework. The upper $\mathcal{H}_\infty$ norm bound of the system including $\mathcal{H}_\infty$ sub optimal controller is used as the performance index. As a case study, the method is applied to a real teleoperation system to study the effects of sensory configuration and back-drivability of the mechanism on the performance of the system in tasks which involve different environment impedances. It can be important criteria to design a teleoperator from the control point of view.**

I. Introduction

The difficulty in implementing a teleoperation system comes from the unpredictability of human and environment impedances, communication disturbances, such as time delay, and quantization error. Previous work in the literature focus on the robust controller design to overcome such uncertainties and disturbances from a control point of view. The controllers are designed for a specific haptic device, slave manipulator and task. As the result, the teleoperation system with a well tuned controller can demonstrate its best performance. This approach is applicable when we can pick our favorite mechanism and sensors for the haptic device and the slave manipulator. However, in some applications, there are constraints in designing the mechanisms and choosing the sensors. For example, in the application of minimally invasive surgery, since the slave manipulator works inside the patient through a small port, the size of the actuators and number of sensors are restricted. However, there is no systematic quantitative methodology to compare different teleoperator architectures, or to evaluate design decisions, such as sensory configuration or drive mechanisms, to guide design of the overall teleoperation systems.

The teleoperator architectures can be classified by the number of channels of sensor information used. There are 4 architectures, position to position, impedance two port, admittance two port, and 4-channel. The position to position architecture model uses only position information. The master device and the slave manipulator follow opposite side's position. With this architecture, the interface can be simple, however, exact force reflection is impossible. Two port and 4-channel architectures are more popular, since we can control the position and force simultaneously. There are two types of two port architectures according to the force sensor location. If force sensor is used at the slave manipulator, it is impedance interface. If force sensor is used at the master device, then it is admittance interface. Hannaford used two port network model design framework in which an operator command position and interaction force between slave manipulator and environment is reflected to the operator [1]. He introduced the hybrid matrix, which he discussed how it can be a measure of performance of the teleoperator. Anderson and Spong introduced passivity theory with scattering matrix to overcome time delay for two port interface [2]. The scattering matrix can be a measure of passivity for uncertainty, such as constant time delay. Colgate suggested the achievable impedance range, Z-width as a measure of performance in sampled data system [3]. Adams and Hannaford applied virtual coupling to impedance and admittance interfaces so as to find the Z-width to satisfy unconditional stability [4]. Lawrence defined transparency as an objective of performance to match impedances of human and environment and proved that all four information channels are required for the high levels of transparency [5]. Yokokohji defined new performance index of maneuverability [6]. Cavusoglu suggested new measure of fidelity which is the sensitivity of the transmitted impedance to changes in the environment impedance. This measure was used to design teleoperation controllers [7]. The above mentioned frameworks need assumptions; human and environment are linear and passive, in addition they have difficulty to treat uncertainty of the plant, disturbance, and noise systematically.

Another approach is to use $\mathcal{H}_\infty$ framework or μ synthesis with velocity and force information channels at both directions. Kazerooni developed an $\mathcal{H}_\infty$ framework to design a controller which transmits only force signals at the master and slave robots [8]. Yan and Salcudean suggested a general framework for $\mathcal{H}_\infty$ optimization using motion scaling [9]. Leung applied μ synthesis to design controllers for time delayed teleoperation [10]. With these frameworks, though we can treat exactly the robust stability and robust performance of the system with multiple sources of uncer-

0-7803-8463-6/04/$20.00 ©2004 IEEE

tainties, this approach are not generally used since a teleoperator has unique characteristics distinguished from other robotic system. In common robotic systems, they have desired path or impedance so that the controller is designed to follow them. However, a teleoperator includes human operator and environment and their impedance is not measurable. In the three approaches referred above, controllers are designed for a specific environment impedance and they have no general methodology for other performance objectives. If the impedance is changed, then controllers are not optimal anymore and the stability can not be guaranteed.

In this paper, we present '*quantitative*' method to compare teleoperator mechanisms and architectures using a task based desired performance. We apply $\mathcal{H}_\infty$ design framework in which the uncertainty of environment impedance, plants, and noise of sensors are treated as disturbance inputs. In this paper, all 4 architectures mentioned and back-drivability of the mechanism are the subject of comparison. The γ value, the upper $\mathcal{H}_\infty$ norm bound of the system including $\mathcal{H}_\infty$ sub-optimal controller, is used as the performance index.

The teleoperator architecture models will be presented in section II followed by the introduction of the $\mathcal{H}_\infty$ framework in section III. The procedure to quantitatively compare teleoperator using $\mathcal{H}_\infty$ framework will be described in section IV. The comparison methodology to practical case will be applied in section V. Section VI will present the quantitative comparison results of teleoperators followed by the discussion in section VII.

II. Teleoperator Architecture Models

In this study, we will consider the 4 different teleoperator architectures shown in Fig.1. Position and force measurements are the most frequently used signals in teleoperation systems. Position sensors are used both at the master device and the slave manipulator in all the configuration in Fig.1. On the other hand, each configuration has different number of force sensors. The interfaces have the following sensor combinations; force sensor at the slave side only (Fig.1(a)), force sensors at both sides (Fig.1(b)), no force sensor (Fig.1(c)), and force sensor at the master side only (Fig.1(d)) .

The description of elements of a teleoperation system are shown in Table.I. Here, we assume that human position is same as the master device's position, i.e., a rigid master. W_{d_1}, W_{d_2}, W_{d_3}, W_{d_4}, W_{τ_h}, $W_{d_{z_e}}$, $W_{d_{\tau_h}}$, and $W_{d_{\tau_e}}$ are the weighting functions to shape and amplify unit random inputs, $\hat{d}_1$, $\hat{d}_2$, $\hat{d}_3$, $\hat{d}_4$, $\hat{\tau}_h$, $\hat{d}_{z_e}$, $\hat{d}_{\tau_h}$, and $\hat{d}_{\tau_e}$ into actual inputs, d_1, d_2, d_3, d_4, τ_h, d_{z_e}, d_{τ_h}, and d_{τ_e}.

III. $\mathcal{H}_\infty$ Design Framework

In this section, the suggested 4 interfaces will be rearranged to the linear fractional (LFT) form [11]. After rearrangement we can get the form as shown in Fig.2, where G is the plant expressed by a state space representation, K is the controller, z is the cost functions to

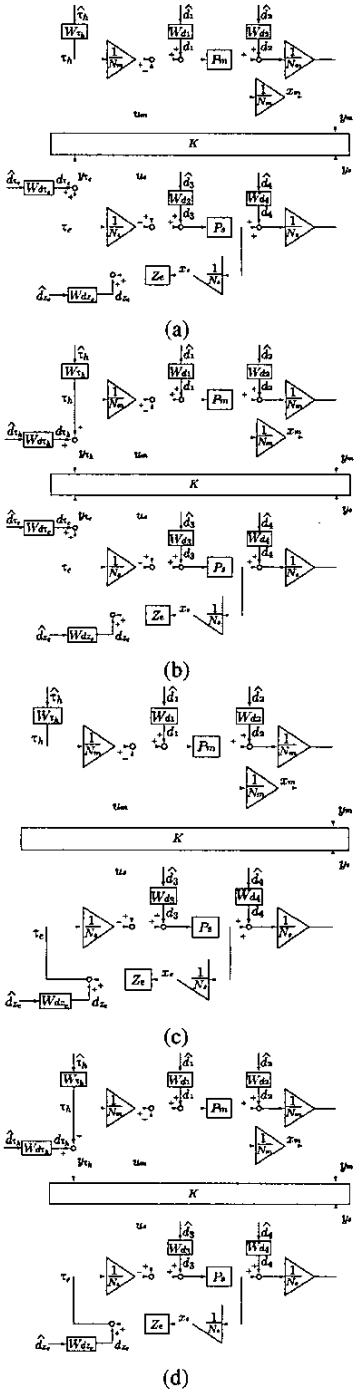

Fig. 1. Teleoperators (a) : with force sensor only at slave side, (b) : with force sensors at both sides, (c) : without force sensor, (d) : with force sensor only at master side.

TABLE I

ELEMENTS OF A TELEOPERATION SYSTEM

P_m, P_s	Nominal plant model of the master and slave
$\hat{Z}_e$	Nominal environment impedance
N_m, N_s	Gear ratios of the master and slave
d_1, d_3	Uncertainties of master and slave expressed as disturbances
d_2, d_4	Sensor noise at master and slave side
d_{ze}	Uncertainty of environment
τ_h	Human operator force command
x_m, x_s	Position of master and slave
u_m, u_s	Control inputs at master and slave
K	$\mathcal{H}_\infty$ optimal controller
y_m, y_s	Position sensor signals
y_{τ_h}, y_{τ_e}	Force sensor signals at master and slave
d_{τ_h}, d_{τ_e}	Force sensor noises at master and slave

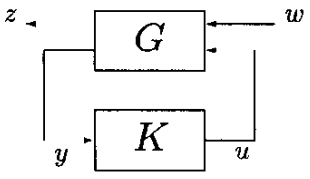

Fig. 2. Linear Fractional Form

measure performance, $\boldsymbol{w}$ is disturbance inputs, $\boldsymbol{y}$ is sensor information, and $\boldsymbol{u}$ is control inputs with

$$\boldsymbol{z} = \left[W_1(\tau_h - \tau_e), \quad W_2(x_m - x_s), \quad W_3 u_m, \quad W_4 u_s\right]^T, \tag{1}$$

$$\boldsymbol{u} = \left[u_m, \quad u_s\right]^T, \tag{2}$$

$$\boldsymbol{w} = \left\{ \begin{array}{c} \left[\hat{d}_1, \quad \hat{d}_2, \quad \hat{d}_3, \quad \hat{d}_4, \quad \hat{d}_{\tau_e}, \quad \hat{\tau}_h, \quad \hat{d}_{z_e}\right]^T \\ \text{for architecture 1} \\ \left[\hat{d}_1, \quad \hat{d}_2, \quad \hat{d}_3, \quad \hat{d}_4, \quad \hat{d}_{\tau_h}, \quad \hat{d}_{\tau_e}, \quad \hat{\tau}_h, \quad \hat{d}_{z_e}\right]^T \\ \text{for architecture 2} \\ \left[\hat{d}_1, \quad \hat{d}_2, \quad \hat{d}_3, \quad \hat{d}_4, \quad \hat{\tau}_h, \quad \hat{d}_{z_e}\right]^T \\ \text{for architecture 3} \\ \left[\hat{d}_1, \quad \hat{d}_2, \quad \hat{d}_3, \quad \hat{d}_4, \quad \hat{d}_{\tau_h}, \quad \hat{\tau}_h, \quad \hat{d}_{z_e}\right]^T \\ \text{for architecture 4} \end{array} \right\}, \tag{3}$$

$$\text{and } \boldsymbol{y} = \left\{ \begin{array}{c} \left[y_m, \quad y_s, \quad y_{\tau_e}\right]^T \text{ for architecture 1} \\ \left[y_m, \quad y_s \quad y_{\tau_h}, \quad y_{\tau_e}\right]^T \text{ for architecture 2} \\ \left[y_m, \quad y_s,\right]^T \text{ for architecture 3} \\ \left[y_m, \quad y_s, \quad y_{\tau_h}\right]^T \text{ for architecture 4} \end{array} \right\}. \tag{4}$$

The first element of the cost function, $\boldsymbol{z}$, is the force tracking performance which evaluates how precisely the master device reflects the interaction force between the slave manipulator and the environment. The second one is the position tracking error. The third and forth ones are the penalties on controller outputs which are inputs to the plant $\boldsymbol{G}$. W_1, W_2, W_3, and W_4 are the frequency dependent weighting functions. Here, we need to explain the first element of the cost function. There are two kinds of force tracking measures typically used in the literature,

$$e_{\tau_1} = \tau_h - \tau_e, \tag{5}$$

and

$$e_{\tau_2} = u_m - \tau_e. \tag{6}$$

In [8], e_{τ_1} is used for force tracking performance. In [9] and [10], e_{τ_2} is used. If e_{τ_2} goes to zero, it means that a controller just reflects the interaction force at the slave side so that u_m becomes τ_e and the operator feels τ_e and impedance of master device. If e_{τ_1} goes to zero, then τ_h follows τ_e. It means that u_m reflects the interaction force, τ_e, and also generate feed forward input to the master device. At a result, the operator does not feel the master device impedance. In this paper, since we will compare various mechanisms, e_{τ_1} should be used in order to keep the operator from feeling the master device impedance. If e_{τ_2} is used for the performance index, then high gear ratio mechanism would have small position variation for the same magnitude of force command resulting in an erroneous reduction of position error.

In this paper, the controller will be designed using the $\mathcal{H}_\infty$ optimization. Then we can find a sub-optimal $\mathcal{H}_\infty$ controller, $\boldsymbol{K}$, such that

$$||\boldsymbol{T}_{zw}||_\infty = ||\mathcal{F}_l(\boldsymbol{G}, \boldsymbol{K})||_\infty < \gamma \tag{7}$$

where $\boldsymbol{T}_{zw}$ is the transfer function which includes plant G and controller $\boldsymbol{K}$, and γ is the upper bound of the $\mathcal{H}_\infty$ norm of cost function, $\boldsymbol{z}$, with respect to unit random inputs, $\boldsymbol{w}$. $\mathcal{F}_l(\cdot,\cdot)$ is lower LFT. Since finding $\mathcal{H}_\infty$ sub-optimal controller is not the issue of this paper and numerical algorithm to calculate it is already well known, we will not explain the details of the solution process. Internally stable $\mathcal{H}_\infty$ sub-optimal controller and γ value can be obtained easily using above LFT form and MATLAB μ-Analysis and Synthesis Toolbox [12].

IV. Analysis Method

In this section, we will summarize how to compare the teleoperators quantitatively using the measurable index, γ value as follows.

1) Select a plant. Specify the nominal plant model, P_m and P_s, modelling error, W_{d_1} and W_{d_3}, and sensor noise, W_{d_2} and W_{d_4}.
2) Specify the range of human force, W_{τ_h}, suitable for the task.
3) Specify nominal environment impedance, Z_e, and uncertainty, $W_{d_{z_e}}$, also based on the task.
4) Specify force sensor noise, $W_{d_{\tau_h}}$ and $W_{d_{\tau_e}}$.
5) Decide the frequency range where performance objectives should be significantly satisfied, $\bar{W}_1$ and $\bar{W}_2$ which have unit magnitudes.
6) Decide actuator limitation, W_3 and W_4.
7) For every interface of teleoperator and various gear ratios, N_m and N_s :
   7-1) Rearrange the system equation into the linear fractional transformation forms

7-2) Calculate the $\mathcal{H}_\infty$ sub-optimal controller, K, and the upper bound of $||T_{zw}||_\infty$, γ, increasing the scales (β_1 and β_2) of $W_1 = \beta_1\tilde{W}_1$ and $W_2 = \beta_2\tilde{W}_2$, until the $\mathcal{H}_\infty$ upper bound becomes equal to 1. In other words, find the β_1 and β_2 values such as

$$\inf\{\frac{1}{\beta_1}, \frac{1}{\beta_2} : ||T_{zw}||_\infty < 1, W_1 = \beta_1\tilde{W}_1, W_2 = \beta_2\tilde{W}_2\}. \tag{8}$$

We can then compare the different teleoperator architectures using the inverse of, β_1 and β_2, the scales of W_1 and W_2 which give best possible performance for the selected mechanism and interface.

V. Case Study

In this section, we will perform a case study to illustrate the analysis method presented above. First, we will introduce the practical plant, disturbances, environment impedance, uncertainty, human force source and noise models that will be used in the subsequent analysis. The y-axis of PHANToM will be used as the master and slave plant models. The y-axis transfer function of PHANToM is given[1] for the master and slave plants as follows [13]:

$$\frac{1}{N^2}P_m = \frac{1}{N^2}P_m = P'_m = P'_s$$

$$= \frac{1}{s^2}\frac{s^4+30.25s^3+2.923\times10^5s^2+5.741\times10^6s+1.784\times10^{10}}{1.526s^2+233s+2.848\times10^5}. \tag{9}$$

In Eq.(9), P'_m and P'_s are nominal model of PHANToM. In Fig.1, P_m and P_s are transfer functions for unit gear ratio. Since PHANToM has a gear ratio $N = 115/10$,

$$P_m = P_s$$

$$= \frac{(11.5)^2}{s^2}\frac{s^4+30.25s^3+2.923\times10^5s^2+5.741\times10^6s+1.784\times10^{10}}{1.526s^2+233s+2.848\times10^5}. \tag{10}$$

Uncertainty expressed as disturbances caused by modelling error and friction are denoted by d_1 and d_3. In this case study, we will only consider the friction of the manipulator. PHANToM has $0.04(N)$ end-effector friction [14]. Therefore, the amplitude of the disturbances are :

$$|d_1| = |d_3| = 0.04(N) \times \frac{10}{115} = 0.003478(N). \tag{11}$$

In H_∞ framework, the disturbances are assumed to be unit magnitude white noise inputs. we used the following filters to convert the unit disturbance inputs to actual disturbances described above.

$$W_{d_1} = W_{d_3} = |d_1| = |d_3|. \tag{12}$$

Sensor noises caused by quantization error are denoted by d_2 and d_4. The forward kinematics of PHANToM y-axis is

$$y = l_2 - l_2\cos(\theta_3) + l_1\sin(\theta_2), \tag{13}$$

where, $l_1 = 215(mm)$ and $l_2 = 170(mm)$ are the lengths of the 2nd and 3rd links, and θ_2 and θ_3 are the corresponding joint angles. Therefore, the relation between actuator angles, θ'_2 and θ'_3, and the joint angles are as follows :

$$\theta_2 = \frac{1}{N}\theta'_2 \text{ and } \theta_3 = \frac{1}{N}\theta'_3. \tag{14}$$

And the variation of forward kinematics is

$$\delta y = N\{l_2\sin(\theta_3)\delta\theta'_3 + l_1\cos(\theta_2)\delta\theta'_2\}. \tag{15}$$

The quantization error of joint position measurement is $2\pi/8192$ rad with 2048 pulses/rev rotary encoder with quadrature encoding. Therefore, the worst quantization error in task space, δy happens where $\theta_2 = 0$, $\theta_3 = \pi/2$. The amplitude of d_2 and d_4 can be calculated as

$$|\delta y|_{\delta\theta'_2=\delta\theta'_3=\frac{2\pi}{8192},\theta_2=0,\theta_3=\pi/2} = |2.568\times10^{-2}|$$
$$= \frac{1}{N}|d_2| = \frac{1}{N}|d_4|, \tag{16}$$

$$|d_2| = |d_4| = 2.953\times10^{-1}(mm). \tag{17}$$

d_2 and d_4 are the quantization errors which are modelled as white noise, therefore, W_{d_2} and W_{d_4} are just amplifiers,

$$W_{d_2} = W_{d_4} = |d_2| = |d_4|. \tag{18}$$

In the set up, the human operator uses his fingertip for force commands. We assume that the human operator force input range, $|\tau_h|$, is $1(N)$ and its bandwidth is below 5 Hz. So,

$$W_{\tau_h} = |\tau_h| \cdot \frac{5\times2\pi}{s+5\times2\pi}. \tag{19}$$

For the nominal environment impedance, we will use the impedance of a silicon gel, which has consistency similar to human soft tissue as reported by [15], and an object which has 30 times higher impedance than a silicon gel.

$$\hat{Z}_e = \left\{\begin{matrix}0.35(0.05s+1) \text{ for silicon gel}\\ 10.50(0.05s+1) \text{ for high impedance env.}\end{matrix}\right\}. \tag{20}$$

The uncertainty of the environment is expressed by disturbance form and its magnitude, $|d_{z_e}|$, is assumed as $0.1(N)$, 10% of human force command. Then,

$$W_{d_{z_e}} = |d_{z_e}| = \frac{1}{10}. \tag{21}$$

Therefore, our task covers $\hat{Z}_e$ with $1/10(N)$ uncertainty in whole frequency. Force sensor noises are denoted by d_{τ_h} and d_{τ_e}. The amplitude of these values are $1/40(N)$ when a $20(N)$ capacity force sensor is used [16]. d_{τ_h} and d_{τ_e} model force sensor noise and W_{d_τ} and $W_{d_{\tau_2}}$ are also just amplifiers,

$$W_{d_\tau} = W_{d_{\tau_2}} = |d_\tau| = |d_{\tau_2}|. \tag{22}$$

VI. Comparison of Teleoperators

This section shows the quantitative comparison results using the procedure mentioned in section IV. The Fig.3 shows the best performance, $(1/\beta_1)$ and $(1/\beta_2)$, of four teleoperator architectures in contact with the silicon gel environment, with respect to various master and slave gear ratios. Fig.4 shows the result for the high impedance environment. In Fig.3 and Fig.4, there are two figure sets which are the results of position and force tracking error,

[1] In this report, dimensions are millimeters for position and Newtons for force.

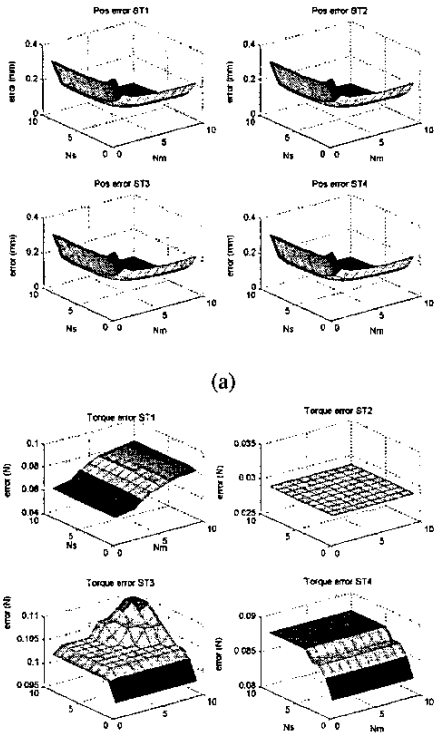

(a)

(b)

Fig. 3. Performance with the silicon gel environment (a) : Position error, (b) : Force error. In each set, the upper left is for architecture Fig.1(a), the upper right for Fig.1(b), the lower left for Fig.1(c), and lower right for Fig.1(d).

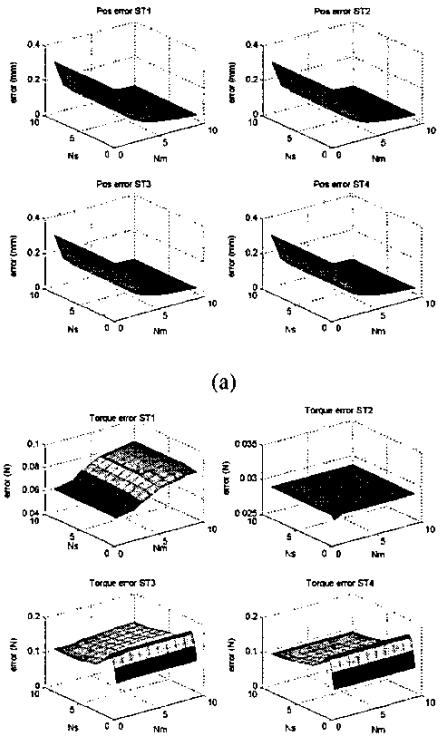

(a)

(b)

Fig. 4. Performance with the high impedance environment (a) : Position error, (b) : Force error. In each set, the upper left is for architecture Fig.1(a), the upper right for Fig.1(b), the lower left for Fig.1(c), and lower right for Fig.1(d).

(a) and (b) respectively. N_m and N_s indicate the gear ratio of master device and slave manipulator. In each sets, there are 4 results according to the architectures. The upper left picture of each figure sets is for the interface in Fig.1(a). The upper right, the lower left, and the lower right one are for Fig.1(b), Fig.1(c), and Fig.1(d), respectively. For example, the upper left picture of Fig.3(a) indicates the minimum upper bound of position tracking error, or the best position tracking performance, of the interface with force sensor only at the slave manipulator with respect to various gear ratios of the master device and slave manipulators. For the task for the soft environment, higher gear ratios at both sides have an advantage of position tracking performance and the architecture is not relevant to the position tracking performance (Fig.3(a)). However, force tracking performance is dependant to the architecture type as well as the gear ratio (Fig.3(b)). For a given architecture the lower gear ratio results in better force tracking performance, however, the gear ratio of the side where the force sensor is attached does not affect the performance. For example, the upper left picture in Fig.3(b) shows that the lower gear ratio at the master side results in a lower force tracking error, while the performance is not affected by the gear ratio at slave side.

For the high impedance environment, the position tracking error gets lower when the gear ratio at master side gets higher, while the gear ratio at the slave side makes no difference (Fig.4(a)). Since the impedance is high, position variation of the slave manipulator becomes very small and the gear ratio at the slave manipulator does not affect the position tracking performance as much. Though Fig.4(b) shows similar results as in Fig.3, except when there is no force sensor at the slave manipulator, the result is not monotonous and there is some intermediate gear ratio that result in worse performance than higher gear ratio.

VII. Discussion

This paper presents a quantitative methodology to compare teleoperation system in the viewpoint of $\mathcal{H}_\infty$ optimality. 4 different teleoperator architectures are classified by sensory configurations, and back-drivability is expressed by gear ratio. The models used include an extensive set of disturbances, and uncertainties of plant and environment are included in the form of disturbances. The most popular haptic device, PHANToM, is used as the master device and the slave manipulators, and practical disturbances are used in the analysis. The results shows the effects of various interface and back-drivability parameters on two

kinds of environments, silicon gel and high impedance object. The method presented provides a quantitative help to design teleoperation systems which is optimal in the sense of task based performance objectives. In the case study, we have considered a limited set for environment uncertainty. It is possible to extend this set. However, this results in an over conservative controller, limiting the nominal performance. In the future, we will treat the environment as the structured uncertainty. It is expected to be a more effective approach to interpret the relation between conservativeness and performance.

ACKNOWLEDGMENT

This research was supported in part by National Science Foundation under grants CISE IIS-0222743 and CISE EIA-0329811, USA, by a grant(02-PJ3-PG6-EV04-0003) of Ministry of Health and Welfare, Republic of Korea, by the International Cooperation Research Program (M6-0302-00-0009-03-A01-00-004-00) of the Ministry of Science and Technology, Republic of Korea, by the National Research Laboratory (NRL) Program (M1-0302-00-0040-03-J00-00-024-00) of the Ministry of Science and Technology, Republic of Korea, and by a grant(M1-0214-00-0116) of the Ministry of Science and Technology, Republic of Korea.

REFERENCES

[1] B. Hannaford, "A design framework for teleoperators with kinesthetic feedback," *IEEE Transactions on Robotics and Automation*, vol. 5, no. 4, pp. 426–434, 1989.

[2] R. J. Anderson and M. W. Spong, "Bilateral control of teleoperators with time delay," *IEEE Transactions on Automatic Control*, vol. 34, no. 5, pp. 494–501, 1989.

[3] J. E. Colgate and J. M. Brown, "Factors affecting the z-width of a haptic display," in *Proceedings of the IEEE Interational Conference on Robotics and Automation*, May 1994, pp. 3205–3210.

[4] R. J. Adams and B. Hannaford, "Stable haptic interaction with virtual environment," *IEEE Transactions on Robotics and Automation*, vol. 15, no. 3, pp. 465–474, 1999.

[5] D. A. Lawrence, "Stability and transparency in bilateral teleoperation," *IEEE Transactions on Robotics and Automation*, vol. 9, no. 5, pp. 624–637, 1993.

[6] Y. Yokokohji and T. Yoshikawa, "Bilateral control of master-slave manipulators for ideal kinesthetic coupligng-formulation and experiment," *IEEE Transactions on Robotics and Automation*, vol. 10, no. 5, pp. 605–620, 1994.

[7] M. C. Cavusoglu, A. Sherman, and F. Tendick, "Design of bilateral teleoperation controllers for haptic exploration and tele manipulation of soft environment," *IEEE Transactions on Robotics and Automation*, vol. 18, no. 4, pp. 641–647, 2002.

[8] H. Kazerooni, T. Tsay, and K. Hollerbach, "A controller design framework for telerobotic systems," *IEEE Transactions on Control Systems Technology*, vol. 1, no. 1, pp. 50–62, 1993.

[9] J. Yan and S. E. Salsudean, "Teleoperation controller design using $\mathcal{H}_\infty$ optimization with application to motion-scaling," *IEEE Transactions on Control Systems Technology*, vol. 4, no. 3, pp. 244–258, 1996.

[10] G. M. H. Leung, B. A. Francis, and J. Apkarian, "Bilateral controller for teleoperators with time delay via μ-synthesis," *IEEE Transactions on Robotics and Automation*, vol. 11, no. 1, pp. 105–116, 1995.

[11] K. Zhou and J. C. Doyle, *Essentials of Robust Control*. Prentice Hall, 1998.

[12] G. J. Balas, J. C. Doyle, K. Glover, A. Packard, and R. Smith, *μ-Analysis and Synthesis Toolbox For Use with MATLAB*. The MathWorks, 2001.

[13] M. C. Cavusoglu, D. Feygin, and F. Tendik, "A critical study of the mechanical and electrical properties of the phantom haptic interface and improvement for high performance control," *Presence*, vol. 11, no. 6, pp. 555–568, 2002.

[14] The sensable technology inc. website. [Online]. Available: http://www.sensable.com

[15] A. Sherman, M. C. Cavusoglu, and F. Tendick, "Comparison of teleoperator control architectures for palpation task," in *Proceedings of the ASME Dynamic Systems and Control Division, part of the ASME Internatioal Mechanical Engineering Congress and Exposition(IMECE 2000)*, Nov. 2000, pp. 1261–1268.

[16] Ati force sensor inc. website. [Online]. Available: http://www.ati-ia.com